

## Evolution of radiating fluid spheres in general relativity

L. Herrera, J. Jiménez, and G. J. Ruggeri

*Departamento de Física, Facultad de Ciencias, Universidad Central de Venezuela, Caracas, Venezuela*

(Received 8 February 1980; revised manuscript received 7 April 1980)

A general method to obtain models of nonstatic radiating fluid spheres is given. Through a certain parameter the models are continuously connected to static solutions of Einstein's equations. The procedure leads, with a minimum of additional hypothesis, to a system of three first-order differential equations for quantities evaluated at the surface of the sphere. An integration of this system allows one at once to obtain the profile of the physical variables inside the sphere. A criterion to predict the bounce of the surface appears in a natural way. As illustrations, we have integrated numerically the equations for two different models: The first is derived from the Schwarzschild interior solution and the second from Tolman's solution VI. In the first case bouncing of the surface is impossible but in the second model the bouncing may occur if certain conditions are satisfied.

### I. INTRODUCTION

The extent to which a general-relativistic calculation of collapse<sup>1-8</sup> could be of any use in the study of different stages of stellar evolution is conditioned by the number and character of the simplifying assumptions made when integrating the field equations and also when choosing the equations of state. Unfortunately, integrating the Einstein equations, for realistic equations of state, without any further simplification other than spherical symmetry is extremely difficult. It seems useful then to consider nonstatic models which are relatively simple to analyze but still it is hoped that they may contain some of the essential features of a realistic situation.

We propose in this paper a general method to obtain models which describe nonstatic radiating spheres. Besides the usual boundary and regularity conditions, our models are restricted by a heuristic condition imposed on the density, pressure, and radial velocity of matter.

As a first result one obtains a set of three first-order differential equations for quantities evaluated at the surface of the sphere. This system (hereafter referred to as surface equations) can be integrated (eventually by numerical methods) to give all the information needed to determine the march of the physical variables, modulo the field equations.

Thus, one obtains different families of nonstatic radiating spheres depending on the specific heuristic condition mentioned above. As we shall see, the models reduce to static solutions of the Einstein equations when no radiation is present and the velocity at the surface of the sphere vanishes.

The paper is organized as follows. The field equations and the general conditions, as well as the conventions used, are included in Sec. II. In Sec. III we describe the method to obtain the

models. The surface equations are analyzed in detail in Sec. IV. In Secs. V and VI, two examples are explicitly worked out to illustrate the procedure. In Sec. VII the results are discussed. Some details of intermediate calculations are included in Appendices A and B.

### II. THE FIELD EQUATIONS AND CONVENTIONS

For the sake of completeness we include here a brief résumé of Bondi's approach to study the evolution of gravitating spheres,<sup>9</sup> which is our starting point.

Let us consider a nonstatic distribution of matter which is spherically symmetric. In radiation coordinates,<sup>10</sup> the metric takes the form

$$ds^2 = e^{2\beta}[(V/r)du^2 + 2du dr] - r^2(d\theta^2 + \sin^2\theta d\phi^2),$$

where  $\beta \rightarrow 0$  as  $r \rightarrow \infty$ . Both  $\beta$  and  $V$  are functions of  $u$  and  $r$ . Here  $u \equiv x^0$  is the timelike coordinate,  $r \equiv x^1$  is a null coordinate, and  $\theta$  and  $\phi \equiv x^{2,3}$  are the usual angle coordinates.

In these coordinates the components of the energy-momentum tensor are distinguished by a bar, and differentiations with respect to  $u$  and  $r$  are denoted by subscripts 0 and 1, respectively.

Thus, Einstein's equations are

$$-8\pi\bar{T}_{00} = -\frac{V_0 - 2\beta_0 V}{r^2} - \frac{V}{r^3}(e^{2\beta} - V_1 + 2\beta_1 V), \quad (1)$$

$$-8\pi\bar{T}_{01} = -\frac{1}{r^2}(e^{2\beta} - V_1 + 2\beta_1 V), \quad (2)$$

$$-8\pi\bar{T}_{11} = -4\beta_1/r, \quad (3)$$

$$\begin{aligned} -8\pi\bar{T}_2^2 &= -8\pi\bar{T}_3^3 \\ &= -e^{-2\beta}\left\{2\beta_{01} - \frac{1}{2}r^{-2}[rV_{11} - 2\beta_1 V \right. \\ &\quad \left. + 2r(\beta_{11}V + \beta_1 V_1)]\right\}. \quad (4) \end{aligned}$$

Following Bondi, local Minkowski coordinates  $(t, x, y, z)$  are introduced by

$$dt = e^{\beta}[(V/r)^{1/2} du + (r/V)^{1/2} dr], \quad (5)$$

$$dx = e^{\beta}(r/V)^{1/2} dr, \quad dy = r d\theta, \quad dz = r \sin\theta d\phi.$$

Denoting the Minkowski components of the energy-momentum tensor by a caret we have

$$\bar{T}_{00} = \hat{T}_{00} \left( \frac{e^{2\beta} V}{r} \right),$$

$$\bar{T}_{01} = (\hat{T}_{00} + \hat{T}_{01}) e^{2\beta},$$

$$\bar{T}_{11} = e^{2\beta} \left( \frac{r}{V} \right) (\hat{T}_{00} + \hat{T}_{11} + 2\hat{T}_{01}),$$

$$\bar{T}_2^2 = \bar{T}_3^3 = \hat{T}_3^3 = \hat{T}_2^2.$$

Next one assumes that for an observer moving relative to these coordinates with velocity  $\omega$  in the radial direction, the space contains

- (a) an isotropic fluid of density  $\hat{\rho}$  and pressure  $\hat{P}$ ,
- (b) isotropic radiation of energy density  $3\hat{\sigma}$ ,
- (c) unpolarized radiation of energy density  $\hat{\epsilon}$  traveling in the radial direction.

For this moving observer, the covariant energy tensor is

$$\begin{pmatrix} \hat{\rho} + 3\hat{\sigma} + \hat{\epsilon} & -\hat{\epsilon} & 0 & 0 \\ -\hat{\epsilon} & \hat{P} + \hat{\sigma} + \hat{\epsilon} & 0 & 0 \\ 0 & 0 & \hat{P} + \hat{\sigma} & 0 \\ 0 & 0 & 0 & \hat{P} + \hat{\sigma} \end{pmatrix}.$$

Then a Lorentz transformation readily shows that

$$\bar{T}_{00} = e^{2\beta} \frac{V}{r} \left( \frac{\rho + P\omega^2}{1 - \omega^2} + \epsilon \right), \quad (6)$$

$$\bar{T}_{01} = e^{2\beta} \frac{1}{1 + \omega} (\rho - P\omega), \quad (7)$$

$$\bar{T}_{11} = e^{2\beta} \frac{r}{V} \frac{1 - \omega}{1 + \omega} (\rho + P), \quad (8)$$

$$\bar{T}_2^2 = \bar{T}_3^3 = -P, \quad (9)$$

where

$$\rho = \hat{\rho} + 3\hat{\sigma}, \quad P = \hat{P} + \hat{\sigma}, \quad \epsilon = \hat{\epsilon} \frac{1 + \omega}{1 - \omega}.$$

Note also that from (5) the velocity of matter in the radiative coordinates is given by

$$\frac{dr}{du} = \frac{V}{r} \frac{\omega}{1 - \omega}. \quad (10)$$

Outside the matter, Eqs. (1)–(9) show that

$$\beta = 0, \quad V = r - 2\bar{m}(u), \quad \epsilon = -\frac{\bar{m}_0}{4\pi r(r - 2\bar{m})}, \quad (11)$$

where  $\bar{m}$  is a function of integration depending on  $u$ . This function is the same as the “mass aspect” defined in Ref. 10. In the static case it coincides with the Schwarzschild mass.

Inside the matter, the function  $\bar{m}(u)$  is generalized to  $\bar{m}(u, r)$  by putting everywhere

$$V = e^{2\beta}[r - 2\bar{m}(u, r)]. \quad (12)$$

Substituting (12) into (1) to (4) and using (6) to (9), one obtains

$$\begin{aligned} \frac{\rho + P\omega^2}{1 - \omega^2} + \epsilon &= \frac{r}{V} e^{-2\beta} \bar{T}_{00} \\ &= \frac{1}{4\pi r(r - 2\bar{m})} \left( -\bar{m}_0 e^{-2\beta} + \frac{r - 2\bar{m}}{r} \bar{m}_1 \right), \end{aligned} \quad (13)$$

$$\frac{\rho - P\omega}{1 + \omega} = e^{-2\beta} \bar{T}_{01} = \frac{\bar{m}_1}{4\pi r^2}, \quad (14)$$

$$\frac{1 - \omega}{1 + \omega} (\rho + P) = \frac{V}{r} e^{-2\beta} \bar{T}_{11} = \frac{r - 2\bar{m}}{2\pi r^2} \beta_1, \quad (15)$$

$$\begin{aligned} P = -\bar{T}_2^2 &= -\frac{\beta_{01} e^{-2\beta}}{4\pi} + \frac{1}{8\pi} \left( 1 - \frac{2\bar{m}}{r} \right) \left( 2\beta_{11} + 4\beta_1^2 - \frac{\beta_1}{r} \right) \\ &\quad + \frac{3\beta_1(1 - 2\bar{m}_1) - \bar{m}_{11}}{8\pi r}. \end{aligned} \quad (16)$$

As emphasized by Bondi it is to be noted that, given  $\beta(u, r)$  and  $\bar{m}(u, r)$ , Eqs. (13) to (16) allow the calculations of  $\omega$ ,  $P$ ,  $\rho$ , and  $\epsilon$ .

In this paper the choice of functions  $\beta(u, r)$  and  $\bar{m}(u, r)$  will be restricted only by the conditions<sup>11</sup>

$$\rho \geq 0, \quad -1 < \omega < 1, \quad \bar{m} < \frac{1}{2}r, \quad \beta_1 > 0.$$

As a boundary condition at the outer surface [say  $r = a(u)$ ] of matter one has  $P = 0$ .<sup>12</sup> Also, since  $\beta = 0$  for  $r > a$ , and  $\beta$  should be a continuous function across  $r = a(u)$ , one imposes  $\beta = 0$  at  $r = a(u) - 0$ . The same is not true for  $\bar{m}_1$ , since there may be a discontinuity of density, and so  $\bar{m}_1 \neq 0$  at  $r = a(u) - 0$ .

Finally, the appearance of  $\beta_{01}$ ,  $\beta_{11}$ , and  $\bar{m}_{11}$  in (16) would lead to unacceptable  $\delta$  functions unless

$$-\beta_0 e^{-2\beta} + \left( 1 - \frac{2\bar{m}}{r} \right) \beta_1 - \frac{1}{2} \frac{\bar{m}_1}{r} = 0 \quad \text{at } r = a - 0. \quad (17)$$

In fact, the left-hand side of (17) is zero at  $r = a + 0$  and so, requiring it to be zero at  $r = a - 0$ , we guarantee that its  $r$  derivative across  $r = a$  does not present a  $\delta$  behavior. But the  $r$  derivative of the left-hand side of (17) gives exactly the combination of second derivatives of  $\beta$  and  $\bar{m}$  which appears in (16).

As stressed by Bondi, it seems extremely difficult to choose  $\beta$  and  $\bar{m}$ , so that for each piece of matter, the relations between  $P$ ,  $\rho$ , and energy

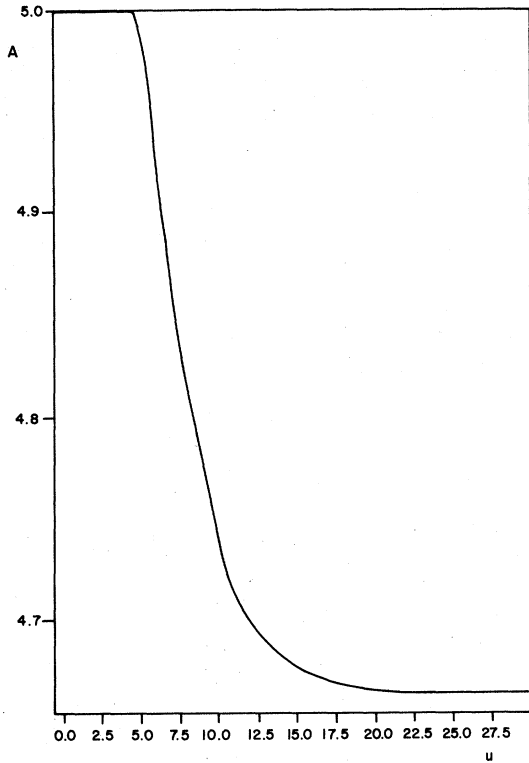


FIG. 1. The radius  $A$  as a function of the timelike coordinate for the initial value  $A|_{u=0}=5$ ,  $\Omega|_{u=0}=1$ . Schwarzschild-type model,  $E \neq 0$ .

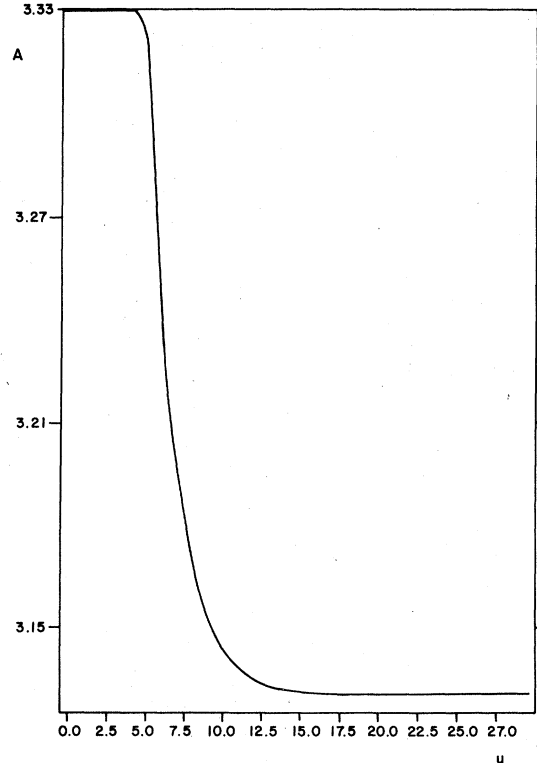


FIG. 2. Same as Fig. 1 but for  $A|_{u=0}=3.33$ ,  $\Omega|_{u=0}=1$ . Schwarzschild-type model,  $E \neq 0$ .

production are in agreement with work on highly compressed matter.

The next section is devoted to presenting a general procedure to construct models satisfying the conditions mentioned above.

### III. THE MODELS

Let us start by noting that because of (14) and (15),

$$\dot{m} = \int_0^r 4\pi r^2 \frac{\rho - P\omega}{1 + \omega} dr, \tag{18}$$

$$\beta = \int_a^r \frac{2\pi r^2}{r - 2\dot{m}} \left( \frac{1 - \omega}{1 + \omega} \right) (\rho + P) dr. \tag{19}$$

Next, let us define the two auxiliary functions (hereafter referred to as effective variables)

$$\bar{\rho} \equiv \frac{\rho - \omega P}{1 + \omega}, \tag{20}$$

$$\bar{P} \equiv \frac{P - \omega \rho}{1 + \omega}. \tag{21}$$

It can be seen at once that  $\bar{\rho} = \rho$  and  $\bar{P} = P$  at  $r = 0$  because  $\omega = 0$  at  $r = 0$ . Also, in the static case  $\bar{P} = P$ ,  $\bar{\rho} = \rho$ .

Finally, note that because of (20) and (21),

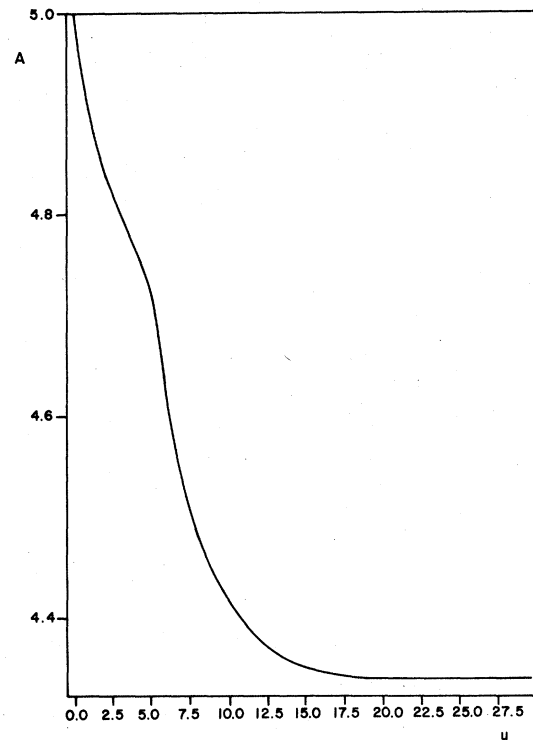


FIG. 3. Same as Fig. 1 but for  $A|_{u=0}=5$ ,  $\Omega|_{u=0}=0.8333$ . Schwarzschild-type model,  $E \neq 0$ .

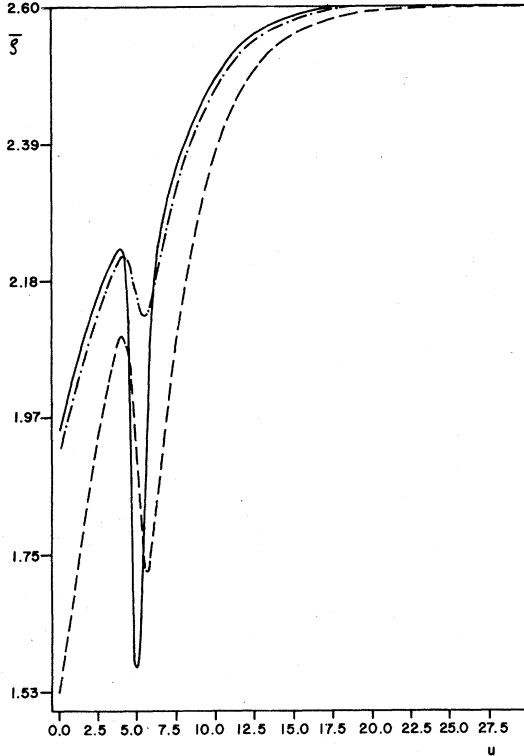


FIG. 4.  $\bar{\rho}$  as a function of the timelike coordinate for the initial data  $A|_{u=0}=5$ ,  $\Omega|_{u=0}=0.83333$  and different pieces of material: Solid line:  $r/a=0$ . Dashed line:  $r/a=1$ . Dot-dashed line:  $r/a=0.4$ . Schwarzschild-type model,  $E \neq 0$ .

$$\bar{m} = \int_0^r 4\pi r^2 \bar{\rho} dr, \quad (18')$$

$$\beta = \int_0^r \frac{2\pi r^2}{r-2\bar{m}} (\bar{\rho} + \bar{P}) dr. \quad (19')$$

Thus,  $\bar{m}$  and  $\beta$  are expressed in terms of  $\bar{\rho}$  and  $\bar{P}$  in the nonstatic case in the same way they are in terms of  $\rho$  and  $P$  in the static case.

These considerations suggest the following procedure to obtain models of radiating contracting spheres.

(1) Take a static interior solution of the Einstein equations for a perfect fluid with spherical symmetry and with given

$$\rho_{\text{static}} = \rho(r), \quad P_{\text{static}} = P(r).$$

(2) Assume that the  $r$  dependence on  $\bar{P}$  and  $\bar{\rho}$  is the same as the  $P_{\text{static}}$  and  $\rho_{\text{static}}$  but being careful with the boundary condition, which now reads, because of (21),

$$\bar{P}_a = -\omega_a \bar{\rho}_a.$$

From now on the subscript  $a$  indicates that the quantity is evaluated at the surface.

(3) With the  $r$  dependence of  $\bar{\rho}$  and  $\bar{P}$  and using

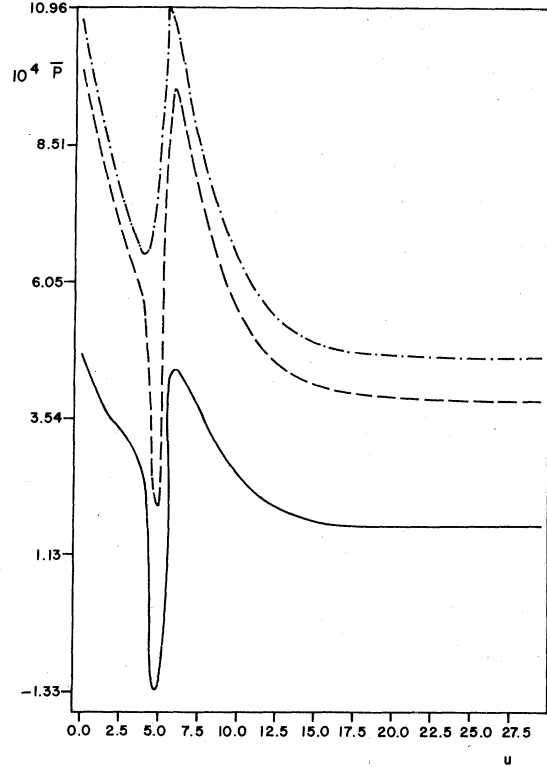


FIG. 5.  $10^4 \bar{P}$  as a function of the timelike coordinates for the initial data  $A|_{u=0}=5$ ,  $\Omega|_{u=0}=0.83333$  and different pieces of material: Dot-dashed line:  $r/a=0$ . Dashed line:  $r/a=0.4$ . Solid line:  $r/a=0.8$ . Schwarzschild-type model,  $E \neq 0$ .

(18') and (19') one gets  $\bar{m}$  and  $\beta$  up to three functions of  $u$ , which will be specified below.

(4) For these three functions one has two differential equations, one of which is (17) and the other is

$$P_a = 0 \text{ or } (T_{l;\mu}^{\mu})_a = 0.$$

Another  $u$ -dependent equation can be obtained evaluating (11) at  $r=a+0$ . Thus

$$E(u) \equiv [\epsilon 4\pi r^2]_{r=a+0} = \left[ \frac{\bar{m}_0 r}{(r-2\bar{m})} \right]_{r=a+0}.$$

Thus one has three differential equations for four unknown functions of  $u$ .

(5) Given one of the functions, the system may be integrated for any particular initial data.

(6) Feeding back the result of integration in the expressions for  $\beta$  and  $\bar{m}$ , these two functions are completely determined.

(7) Using (13)–(16),  $\rho$ ,  $P$ ,  $\omega$ ,  $\epsilon$  may be found.

In the above we have outlined the general program for the attainment of models. In the next

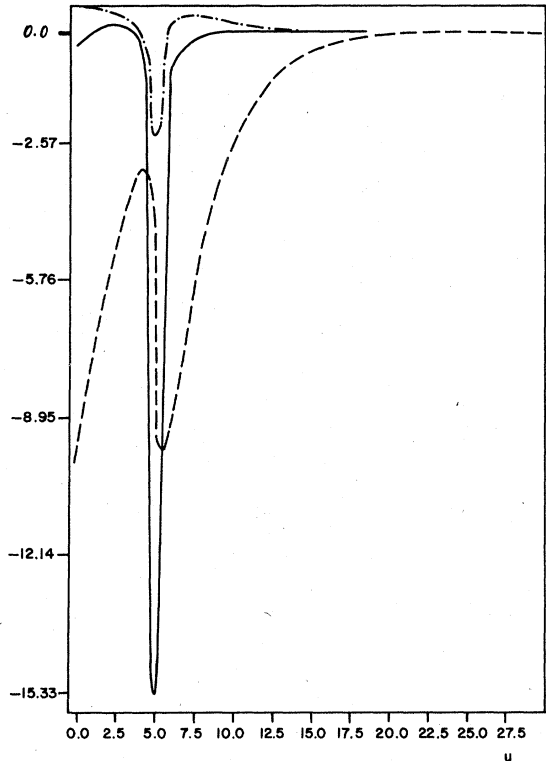


FIG. 6.  $v$  as a function of the timelike coordinates for the initial data  $A|_{u=0} = 5$ ,  $\Omega|_{u=0} = 0.83333$  and different pieces of material: Dot-dashed line:  $r/a = 0.2$ . (The function has been multiplied by a factor  $10^2$ .) Solid line:  $r/a = 0.6$ . (The function has been multiplied by a factor  $10^2$ .) Dashed line:  $r/a = 1$ . (The function has been multiplied by a factor  $10$ .) Schwarzschild-type model,  $E \neq 0$ .

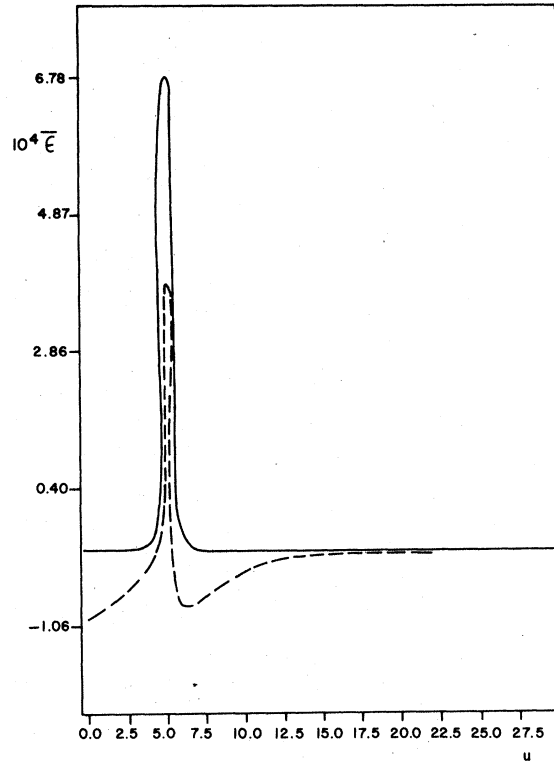


FIG. 7.  $10^4 \bar{\epsilon}$  as a function of the timelike coordinate for the initial data  $A|_{u=0} = 5$ ,  $\Omega|_{u=0} = 0.83333$ , and different pieces of material: Dashed line:  $r/a = 0.2$ . Solid line:  $r/a = 0.1$ . Schwarzschild-type model,  $E \neq 0$ .

section we shall investigate in detail the three differential equations mentioned in point (4).

#### IV. EQUATIONS AT THE SURFACE

##### A. The equations

In this section we show how to construct, with some relatively mild additional assumptions, a complete set of dynamical equations which control the evolution of the physical variables at the surface of the sphere.

To begin with let us consider Eq. (17) and show that it gives no more information than Eqs. (10) and (11) taken at  $r = a$ . In fact, near the surface

$$\beta(r, u) \approx \beta_{1a}(r - a) + \dots,$$

then

$$\beta_{0a} = -\dot{a}\beta_{1a}, \quad \text{with } \dot{a} \equiv \frac{da}{du}.$$

Thus Eq. (17) reads

$$\dot{a} = - \left( 1 - \frac{2m}{a} \right) - \frac{\dot{m}_{1a}}{2a\beta_{1a}}.$$

Here  $m \equiv \dot{m}_a$  is the "total" mass of the object. Using now Eqs. (14) and (15) we arrive at

$$\dot{a} = (1 - 2m/a) \frac{\omega_a}{1 - \omega_a}. \tag{22}$$

We have found it convenient to scale the total mass  $m$ , the radius  $a$ , and the timelike coordinate  $u$ , by the initial mass  $m(u=0) \equiv m(0)$ ,

$$A \equiv a/m(0), \tag{23}$$

$$M \equiv m/m(0), \tag{24}$$

$$u/m(0) \rightarrow u,$$

and to define

$$F = 1 - 2M/A, \tag{25}$$

$$\Omega \equiv \frac{1}{1 - \omega_a}. \tag{26}$$

Equation (22) can then be written as

$$\dot{A} = F(\Omega - 1). \tag{27}$$

A second equation relates the total mass-loss

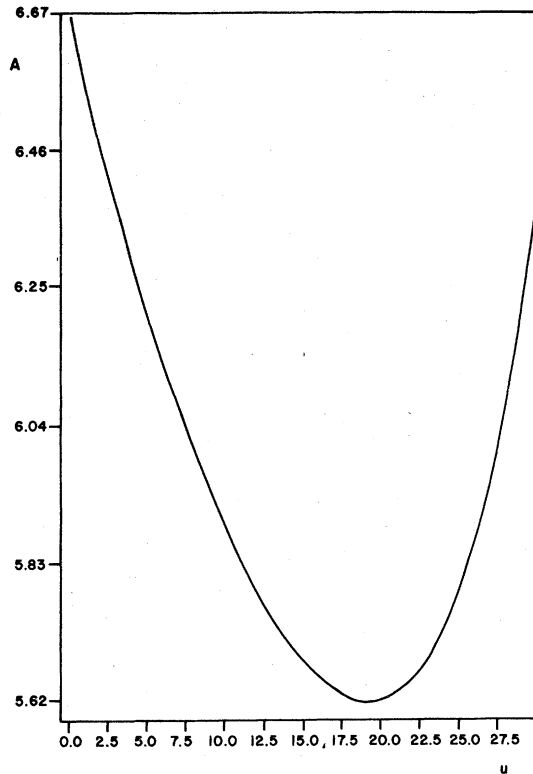


FIG. 8.  $A$  as a function of the timelike coordinate for the initial data  $\Omega|_{u=0}=0.8571$ ,  $A|_{u=0}=6.6666$ . Tolman VI-type model,  $E \neq 0$ .

rate with the energy flux through the surface. This can be obtained by evaluating Eq. (11) for  $r = a + 0$ , and takes the form

$$\dot{M} = -FE, \quad (28)$$

where, as stated in the previous section,

$$E \equiv (4\pi r^2 \epsilon)_a.$$

Equation (28) can be rewritten so that only the surface variables  $A$ ,  $F$ , and  $\Omega$  appear. This is obtained through combination of Eqs. (25) and (27) with (28), and reads

$$\frac{\dot{F}}{F} = \frac{2E + (1-F)(\Omega - 1)}{A}. \quad (29)$$

Equations (27) to (29) are completely general and therefore valid for any model of a spherically symmetric radiative dynamical situation. To specify the dynamics completely for any set initial conditions and a given boundary flux output  $E(u)$ , we need a third equation which relates the surface variables. It will be seen that this can be obtained from the condition  $P_a = 0$ .

We start by recasting the pressure equation (16) in a more suggestive form. Equation (31) below can be obtained either through the use of Eqs. (16),

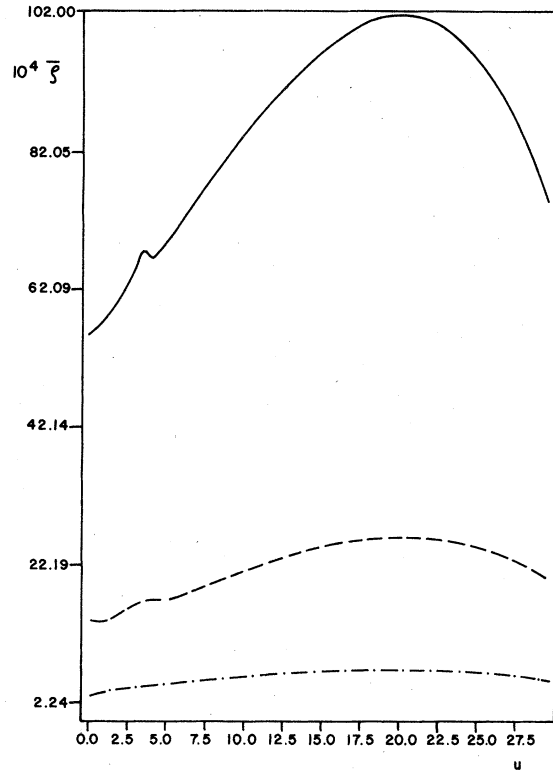


FIG. 9.  $10^4 \bar{\rho}$  as a function of the timelike coordinate for the initial value  $A|_{u=0}=0.6666$ ,  $\Omega|_{u=0}=0.8571$ : Solid line:  $r/a=0.2$ . Dashed line:  $r/a=0.4$ . Dot-dashed line:  $r/a=0.8$ . Tolman VI-type model,  $E \neq 0$ .

(14), and (15) or by appealing to the conservation equation  $T_{1;u}^u = 0$ . This last equation together with Eqs. (20) and (21) leads to

$$-(e^{2\beta} \bar{P})_1 + [(e^{2\beta} r/V)(\bar{\rho} + \bar{P})]_0 + \frac{\beta_1}{2\pi r} \left( -\frac{3}{2} \frac{V}{r^2} - \frac{e^{2\beta}}{2r} + \frac{2V}{r^2(1-\omega)} \right) = 0. \quad (30)$$

Substitution of Eqs. (12) and (14) leads, after some straightforward manipulations, to the form

$$-e^{2\beta} \left( \frac{\bar{P} + \bar{\rho}}{1 - 2\bar{m}/r} \right)_0 + \frac{\partial \bar{P}}{\partial r} + \frac{\bar{P} + \bar{\rho}}{1 - 2\bar{m}/r} \left( 4\pi r \bar{P} + \frac{\dot{m}}{r^2} \right) = \frac{2}{r} (P - \bar{P}). \quad (31)$$

This equation is the generalization of the usual (Tolman-Oppenheimer-Volkov) equation of hydrostatic support, for nonstatic radiative situations. We stress the conspicuous role played by the effective variables  $\bar{\rho}$ ,  $\bar{P}$ .

At the surface, where  $\bar{P}_a = -\omega_a \bar{\rho}_a$ , Eq. (31) reduces to

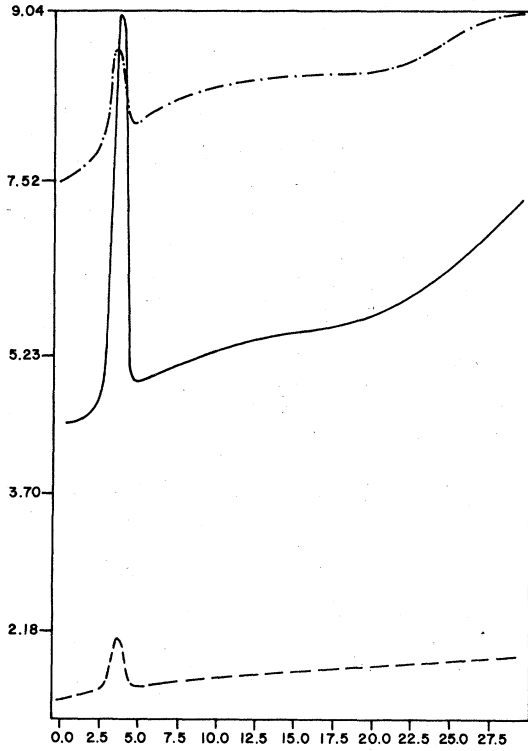


FIG. 10.  $\bar{\epsilon}$  as a function of the timelike coordinate for the initial data  $\Omega|_{u=0}=0.8571$ ,  $A|_{u=0}=6.6666$  and different pieces of material: Dot-dashed line:  $r/a=0.2$ . Dashed line:  $r/a=0.4$ . Solid line:  $r/a=0.6$ . (The function  $\bar{\epsilon}$  is multiplied by 10.) Tolman VI-type model,  $E \neq 0$ .

$$-\left(\frac{\bar{\rho} + \bar{P}}{1 - 2\bar{m}/r}\right)_{0a} + \left(\frac{\partial \bar{P}}{\partial r}\right)_a + \left[\left(\frac{\bar{\rho} + \bar{P}}{1 - 2\bar{m}/r}\right) \left(4\pi r \bar{P} + \frac{\bar{m}}{r^2}\right)\right]_a = \frac{2\omega_a \bar{\rho}_a}{a}, \quad (32)$$

on which we shall elaborate in what follows. Consider first the time derivative in Eq. (32). We have

$$\left(\frac{\bar{P} + \bar{\rho}}{1 - 2\bar{m}/r}\right)_{0a} = \frac{(\bar{P} + \bar{\rho})_{0a}}{F} + \frac{2}{aF^2} (\bar{\rho}_a + \bar{P}_a) \dot{m}_{0a}, \quad (33)$$

but

$$\dot{m}_{0a} = \dot{m} - \dot{a} \bar{m}_{1a} \quad (34)$$

$$\left(\frac{\bar{\rho} + \bar{P}}{1 - 2\bar{m}/r}\right)_{0a} = -\left(\frac{\bar{\rho}_a}{\Omega F}\right) \left[\left(\frac{\dot{F}}{F} + \frac{\dot{\Omega}}{\Omega} - \frac{\dot{\bar{\rho}}_a}{\bar{\rho}_a}\right) - (\Omega - 1)(1 - F)/a\right] - F(\Omega - 1) \left[\frac{2\bar{\rho}_a}{\Omega a F^2} \dot{m}_{1a} + (\bar{P} + \bar{\rho})_{1a}/F\right] \quad (37)$$

if  $\rho_a \neq 0$ . If the density at surface is zero, the expression is

$$\left(\frac{\bar{\rho} + \bar{P}}{1 - 2\bar{m}/r}\right)_{0a} = -(\Omega - 1)(\bar{\rho} + \bar{P})_{1a}. \quad (38)$$

To give a compact form to (31) we found it useful

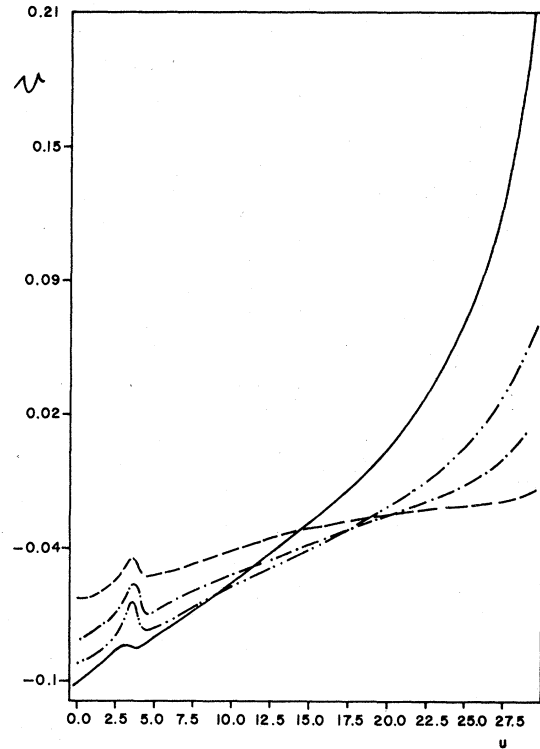


FIG. 11.  $v$  as a function of the timelike coordinate for the initial data  $A|_{u=0}=6.6666$ ,  $\Omega|_{u=0}=0.8571$  and different pieces of material: Dashed line:  $r/a=0.2$ . Dot-dashed line:  $r/a=0.4$ . Double dot-dashed line:  $r/a=0.6$ . Solid line:  $r/a=1$ . Tolman VI-type model,  $E \neq 0$ .

and

$$(\bar{\rho} + \bar{P})_{0a} = [(\bar{P} + \bar{\rho})_{r=a}]_0 = \dot{a}(\bar{P} + \bar{\rho})_{1a} = [\bar{\rho}_a(1 - \omega_a)]_0 - \dot{a}(\bar{P} + \bar{\rho})_{1a}. \quad (35)$$

Combining these three last equations we arrive at

$$\left(\frac{\bar{P} + \bar{\rho}}{1 - 2\bar{m}/r}\right)_{0a} = \frac{2(\bar{P}_a + \bar{\rho}_a)}{aF^2} \dot{m} + \frac{1}{F} \left(\frac{\rho_a}{\Omega}\right)_0 - \dot{a} \left[\frac{2(\bar{P}_a + \bar{\rho}_a)}{aF^2} \bar{m}_{1a} + \frac{(\bar{P} + \bar{\rho})_{1a}}{F}\right]. \quad (36)$$

$\dot{m}$  and  $\dot{a}$  can be eliminated through the use of (27)–(29) and we get

to define the quantity

$$\bar{R}(u) \equiv \left[\frac{\partial \bar{P}}{\partial r} + \frac{\bar{P} + \bar{\rho}}{(1 - 2\bar{m}/r)} \left(4\pi r \bar{P} + \frac{\bar{m}}{r^2}\right)\right]_a \quad (39)$$

which is a function of time whose structure depends ultimately on the equation of state. Then if

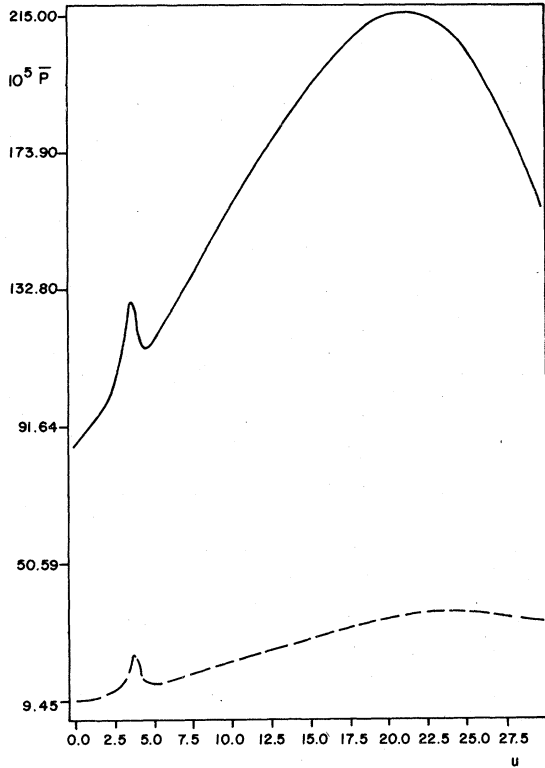


FIG. 12.  $\bar{P}10^5$  as a function of the timelike coordinate for the initial data  $A|_{u=0} = 6.6666$ ,  $\Omega|_{u=0} = 0.8571$  and different pieces of material: Solid line:  $r/a = 0.2$ . Dashed line:  $r/a = 0.8$ . (The function  $\bar{P}10^5$  is multiplied by 10.) Tolman VI-type model,  $E \neq 0$ .

$\bar{\rho}_a$  is not zero, Eq. (31) can be written, after multiplying through by  $-\Omega F/\bar{\rho}_a$  and doing some rearrangement, as

$$\frac{\dot{F}}{F} + \frac{\dot{\Omega}}{\Omega} - \frac{\dot{\bar{\rho}}_a}{\bar{\rho}_a} + \frac{\Omega^2 F \ddot{R}}{\bar{\rho}_a} + (\Omega - 1) \left[ 4\pi a \bar{\rho}_a \frac{(3\Omega - 1)}{\Omega} - \frac{3+F}{2a} + \frac{\Omega F}{\bar{\rho}_a} \bar{\rho}_{1a} \right] = 0. \quad (40)$$

If  $\bar{\rho}_a = 0$ , then Eq. (31) reduces to

$$[\Omega \bar{P}_1 + (\Omega - 1) \bar{\rho}_{1a}]_a = P_{1a} = 0. \quad (41)$$

To proceed further we obviously need more detailed information about the relation of the physical variables  $\bar{\rho}$ ,  $\bar{P}$  and their dependence on  $u$  and  $r$ . The possibilities are of course very ample and so in the following sections we shall limit ourselves to a detailed study of two relatively simple models. For these two models the effective density is separable, i.e.,  $\bar{\rho} = f(u)h(r)$  and so

$$\begin{aligned} \bar{m} &= \frac{1}{2} a (1 - F) = f(u) \int_0^a 4\pi r^2 h(r) dr \\ &= \bar{\rho}_a \int_0^a 4\pi r^2 h(r) dr / h(a). \end{aligned} \quad (42)$$

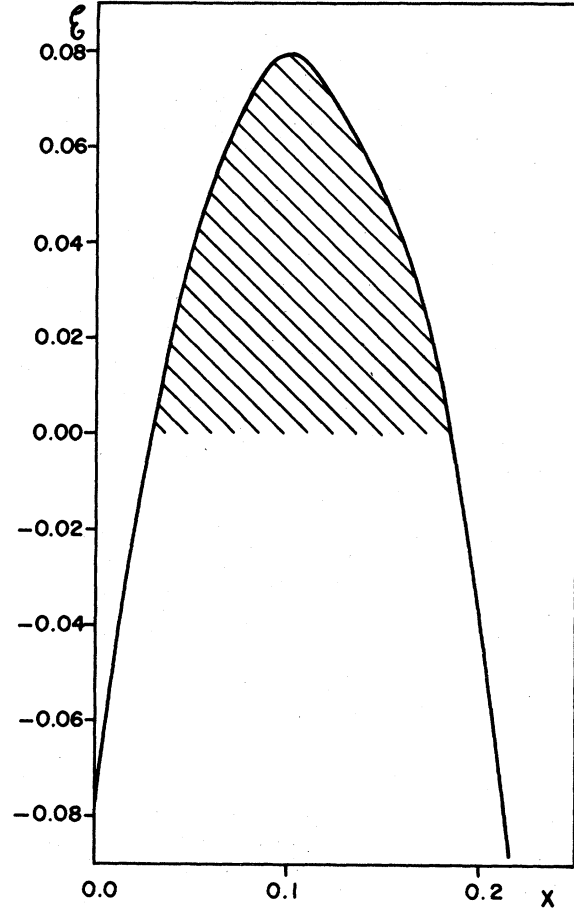


FIG. 13. The quantity  $\mathcal{G}(x) = x(3-14x) - 8E$  with  $x = M/A$  for  $E = 0.01$  in the Tolman VI-type model. Bouncing can occur only within the dashed region.

Then

$$-\frac{\dot{\bar{\rho}}_a}{\bar{\rho}_a} = \frac{\dot{F}}{1-F} + k(a)F(\Omega - 1), \quad (43)$$

where

$$k(a) = \frac{d}{da} \ln \left( \frac{1}{a} \int_0^a dr r^2 h(r) / h(a) \right). \quad (44)$$

Substitution of this into Eq. (40) provides the third dynamical equation for the surface variables. It takes the form

$$\frac{\dot{F}}{F} + (1-F) \frac{\dot{\Omega}}{\Omega} = G(F, \Omega, A), \quad (45)$$

where

$$\begin{aligned} G &= -\frac{\Omega^2 F(1-F)}{\bar{\rho}_a} \frac{\ddot{R}}{R} \\ &+ (F-1)(\Omega-1) \left[ \frac{4\pi a}{\Omega} (3\Omega-1) \bar{\rho}_a \right. \\ &\quad \left. - \frac{(3+F)}{2a} + \frac{\Omega F}{\bar{\rho}_a} \bar{\rho}_{1a} + k(a)F \right]. \end{aligned} \quad (46)$$

In Eq. (45) the fact has been advanced that for the models considered below,  $G$  can be expressed solely in terms of the surface variables  $F$ ,  $\Omega$ , and  $A$ . This implies that Eqs. (27), (29), and (45) constitute a complete set of coupled nonlinear dynamical equations for the surface variables. The models considered below are such that all the dynamics is contained in these surface variables which control then the behavior of the different pieces of matter inside the spherical body.

#### B. Bouncing at the surface

Some interesting conclusions can be obtained even at this level of generality. One of these conclusions concerns the possibility of bouncing at the surface of the body under the combined action of gravity and incoherent radiation. This, of course, is related to the occurrence of a minimum of the object's radius  $A$  during the evolution. According to Eq. (27) this requires, as expected,  $\Omega = 1$  and we have

$$\ddot{A} = F\dot{\Omega},$$

which together with Eqs. (29) and (45) gives

$$\ddot{A} = \frac{F}{1-F} \left( G - \frac{2E}{A} \right). \quad (47)$$

All quantities are to be evaluated at the extremal point. Two immediate consequences follow from Eq. (47). The first one is that a positive flux of energy tends to decrease the radius of the sphere, i.e., it favors the compactation of the object, which is easily understandable. The same happens when  $G < 0$ . Of course, the opposite effect occurs when these quantities have the opposite signs. A second general consequence is that a radiating sphere can only bounce at its surface when  $G(F, \Omega = 1, A) \geq 0$ . According to (46) this is equivalent to

$$-\tilde{R}(F, A, \Omega = 1) \geq 0. \quad (48)$$

A physical meaning can be associated to this equation as follows. For nonradiating, static configuration,  $\tilde{R}$ , as defined by Eq. (39) when  $\omega = 0$ , consists of two parts. The first term which rep-

resents the hydrodynamical force and the second which is of course the gravitational force. The resulting force in the sense of increasing  $r$  is precisely  $-\tilde{R}$ . If this is positive a net outward acceleration occurs and vice-versa. Equation (48) is the natural generalization of this result for general nonstatic configurations.

In the next section a nonstatic radiating generalization of the internal Schwarzschild model will be studied. This model is such that for  $\omega_a = 0$  ( $\Omega = 1$ ) the material finds itself in an equilibrium configuration irrespective of the value of the other parameters  $F$ ,  $A$ , etc. This is so because  $\tilde{R} = 0$ . In this case, the only driving force is the radiation flux and of course the bouncing of the surface is impossible. In the opposite case, when  $\tilde{R}$  is not identically zero, although the surface is momentarily at rest when  $\Omega = 1$ , the system finds itself in a nonequilibrium configuration which cannot persist even if no radiation is present. A model of this last situation will also be studied below.

#### V. THE SCHWARZSCHILD-TYPE MODEL

Let us now illustrate the method presented above with a very simple model inspired by the well-known Schwarzschild interior solution.

With this aim we take

$$\tilde{\rho} = \begin{cases} f(u), & r \leq a(u) \\ 0, & r > a(u) \end{cases} \quad (49)$$

where  $f$  is an arbitrary function of  $u$  and  $a(u)$  defining the radius of the sphere.

The expression for  $\tilde{P}$  is

$$\frac{\tilde{P} + \frac{1}{3}\tilde{\rho}}{\tilde{P} + \tilde{\rho}} = \left( 1 - \frac{8}{3}\pi\tilde{\rho}r^2 \right)^{1/2} k, \quad (50)$$

where  $k$  is a function of  $u$  to be defined from the boundary condition

$$\tilde{P}_a = -\omega_a f. \quad (51)$$

Thus, (50) and (51) give

$$\tilde{P} = f(u) \left\{ \frac{(1 - 3\omega_a)(1 - \frac{8}{3}\pi fr^2)^{1/2} - (1 - \omega_a)(1 - \frac{8}{3}\pi fa^2)^{1/2}}{3(1 - \omega_a)(1 - \frac{8}{3}\pi fa^2)^{1/2} - (1 - \frac{8}{3}\pi fr^2)^{1/2}(1 - 3\omega_a)} \right\}. \quad (52)$$

Using (18') and (19') it is very easy to obtain expressions for  $\beta$  and  $\tilde{m}$ :

$$\beta = \begin{cases} \frac{1}{2} \ln \left[ (1 - \omega_a) \left( \frac{3(1 - \frac{8}{3}\pi fa^2)^{1/2}}{2(1 - \frac{8}{3}\pi fr^2)^{1/2}} - \frac{1}{2} \right) + \omega_a \right], & r < a \\ 0, & r \geq a \end{cases} \quad (53)$$

$$m = \begin{cases} \frac{4}{3}\pi fr^3, & r \leq a(u) \\ \frac{4}{3}\pi fa^3, & r > a \end{cases}. \quad (54)$$

In order to write down explicitly the surface equations for this model, observe that

$$\tilde{R} = 0$$

for any value of  $f(u)$ . Next, using (44) and (46) one gets

$$k(u) = \frac{2}{a}$$

and

$$G = -3(1-F)^2(\Omega-1)(2\Omega-1)/2a\Omega$$

so that Eq. (45) takes the form

$$\frac{\dot{F}}{F} + (1-F)\frac{\dot{\Omega}}{\Omega} + \frac{3(1-F)^2(\Omega-1)(2\Omega-1)}{2A\Omega} = 0. \quad (55)$$

This last equation, together with (29) and (27), constitutes the differential system for the surface in this model. In order to obtain information from it, we must specify one function of  $u$  and the initial data. Specifically we choose the product  $FE$  to be a Gaussian so that the total radiated mass is  $\frac{1}{10}$  of the initial mass. As for the initial data the following cases were considered:

- (a)  $\Omega|_{u=0} = 1$ ,  $A|_{u=0} = 5$ ,  $F|_{u=0} = 0.6$ ,
- (b)  $\Omega|_{u=0} = 0.83333$ ,  $A|_{u=0} = 5$ ,  $F|_{u=0} = 0.6$ ,
- (c)  $\Omega|_{u=0} = 1$ ,  $A|_{u=0} = 3.33333$ ,  $F|_{u=0} = 0.4$ .

The integration was done numerically for values of  $u$  between 0 and 30 for this set of initial data (this specific interval was suggested by the march of the variables themselves).

Figures 1-3 show the evolution of the radius  $A$ . It is seen immediately that the system tends to a situation of constant radius for the initial data chosen above. For very compact objects  $A^{(u=0)} \leq 3.3333$  and very high inward (initial) velocities  $|dr/du|_{u=0} \geq 0.1$ , the object will collapse and/or the equation of state will be of the type  $P \geq \rho$ .

Feeding back the numerical values of  $A$ ,  $F$ , and  $\Omega$  in (53) and (54) we obtain the complete specification of  $\beta$  and  $\tilde{m}$  for any value of  $r$ . This gives us at once, using the field equations, the functions  $\rho$ ,  $\epsilon$ ,  $P$ , and  $\omega$  for any piece of the material. Specifically, we calculated them for the values  $r/a = 0, 0.2, 0.4, 0.6, 0.8$ , and 1. Further details of these calculations are included in Appendix A.

Figures 4-7 give the profile of the variables versus the timelike coordinate for different pieces of material and for the initial data (b). [Note that instead of  $\omega$ , we work with the quantity  $v \equiv dr/du$ , as defined by Eq. (10)].

The evolution can be briefly described as a transition from a nonstatic configuration to a Schwarzschild solution.

Also observe that although there is no bounce at the surface, some inner regions do bounce as indicated in Fig. 6.

For the initial data (a) and (c) the results are very similar, but in these cases the initial configuration corresponds to a Schwarzschild interior solution.

## VI. TOLMAN VI-TYPE MODEL

As a second example we shall investigate in this section a model obtained from the Tolman VI solution.<sup>13</sup> Unlike the Schwarzschild-type solution this model can present bouncing at the surface since  $\tilde{R} \neq 0$ , and so one expects new interesting situations.

Following the scheme of Sec. III, let us take

$$\tilde{\rho} = \frac{3g(u)}{r^2}, \quad (56)$$

$$\tilde{P} = \frac{g(u)}{r^2} \frac{1-9D(u)r}{1-D(u)r}, \quad (57)$$

where  $g$  and  $D$  are functions of  $u$ .

Substituting (56) and (57) into (18') and (19'), one gets

$$\tilde{m} = 12\pi gr \quad (58)$$

and

$$\beta = \frac{8\pi g}{(1-24\pi g)} \ln \frac{(1-Dr)^2 r}{(1-Da)^2 a}. \quad (59)$$

It is useful to express the function  $D$  in terms of the more physical quantity  $\omega_a$ . Taking into account the boundary conditions

$$\tilde{P}_a = -\omega_a \left( \frac{\rho}{1+\omega} \right)_a = -\frac{3\omega_a g}{a^2} \quad (60)$$

and comparing it with (57) evaluated at the surface one gets

$$D = \frac{1+3\omega_a}{3a(3+\omega_a)}. \quad (61)$$

Using (39), (44), (46), and the expressions for  $\tilde{P}$  and  $\tilde{\rho}$  above, one obtains

$$R = \frac{1}{64\pi a^2} \frac{(1-F)(4-7F)}{\Omega^2 F}, \quad (62)$$

$$k(a) = 2/a, \quad (63)$$

$$G = \frac{1}{8A} (1-F)F(4\Omega-3)(4\Omega-1) - \frac{(1-F)^2}{2\Omega A}. \quad (64)$$

Feeding back (64) into (45) one gets one of the surface equations for this model; the other two equations, as already mentioned, are (27) and (29).

These surface equations were numerically integrated for the following set of initial data (we choose the product  $FE$  to be the same as in the Schwarzschild-type model):

- (a)  $A|_{u=0} = 6.666667$ ,  $\Omega|_{u=0} = 0.857143$ ,  $F|_{u=0} = 0.7$ ,
- (b)  $A|_{u=0} = 5$ ,  $\Omega|_{u=0} = 1$ ,  $F|_{u=0} = 0.6$ .

As for the previous model we performed the integration for  $0 \leq u \leq 30$ .

Figure 8 shows the evolution of the radius of the sphere for the initial data (a). Figures 9-12 give the profiles of the matter variables versus the

timelike coordinates for the same initial data (a) and different pieces of material.

The fact that bounce at the surface may occur should not surprise, since  $\tilde{R}$  is not identically zero. As can be seen from (62),  $-\tilde{R} \geq 0$  if  $F \geq \frac{4}{3}$ . In this case  $F = 1 - 24\pi g = 1 - 2M/a$ , and the condition reads  $g \leq 1/56\pi$  or  $M/a \leq \frac{3}{14}$ . This is in accord with the equilibrium value given by Tolman and confirms the expectation that bouncing may only occur when the gravitational potential is small. Figure 13 depicts graphically the region where a bouncing occurs in terms of the "surface potential"  $x = M/a$ .

The bouncing situation obtained from the initial data (a) presents another interesting aspect, namely, for a long interval of time after the bounce the inner zones continue to contract. The evolution can be pictured as an expanding envelope containing a contracting radiating core (see Figs. 10 and 11).

## VII. CONCLUSIONS

We have seen so far that with relatively mild assumptions it is possible to construct a differential system at the surface which allows one to describe the dynamical situation inside the radiating sphere. The critical assumption in our method appears when identifying the dependence of  $\tilde{P}$  and  $\tilde{\rho}$  with the corresponding dependence of the static case. Although this identification is based on a heuristic argument, two remarks are in order:

(1) In the limit  $\omega \rightarrow 0$  the identification is obviously true so that for small velocities the method may always be expected to work.

(2) In the examples examined above, at least some of the results are close to what one could intuitively expect.

The next thing to do should be to construct models fitting the observational data of some astrophysical phenomena [in this sense, note that our initial data in the two models above was suggested by supernova data ( $v = 0.1$ ; total radiated mass =  $0.1 m(0)$ )].

In relation with this point there is an important question which remains unanswered in the context of the present work, namely, what is the source of the radiation emitted by the models. For the Tolman VI-type model it seems reasonable to think as if the radiation were produced at a singularity at the center of the model. In general, the answer to this question requires the consideration of a specific microscopic process which could fit the conditions and characteristics of the different models.

Also, it is worth mentioning that solutions which do not radiate to the outside ( $E = 0$ ) are physically

questionable, because the energy-momentum tensor [Eqs. (6)–(9)] will not be valid. Moreover, in those cases the condition  $P|_a = 0$  no longer holds, since there exists a discontinuity of the radiation flux across the surface.<sup>12</sup>

Finally, we would like to mention two possible extensions of the method proposed in this paper.

(1) Instead of giving the function  $FE$  to solve the surface equations one could give  $\Omega$ ,  $A$ , or  $F$  depending on the kind of phenomena one would like to describe.

(2) The  $r$  dependence for the variables  $\tilde{P}$  and  $\tilde{\rho}$  could be inferred from a different heuristic argument than the one we have used.

## ACKNOWLEDGMENT

This work was supported in part by C.O.N.I.C.I.T. (Venezuela).

## APPENDIX A

Once the surface equations are integrated for the Schwarzschild-type case it is useful to introduce the following dimensionless auxiliary quantities:

$$Y \equiv e^{2\beta} \equiv \frac{1}{\Omega} \left[ \frac{3}{2} \left( \frac{F}{Z} \right)^{1/2} + \Omega - \frac{3}{2} \right], \quad (A1)$$

$$Z \equiv \left[ 1 - (1-F) \frac{r^2}{a^2} \right].$$

It is now easy to obtain

$$\beta_1 m(0) \equiv \frac{3(1-F)\sqrt{F}}{4\Omega Z^{3/2} Y A} \left( \frac{r}{a} \right), \quad (A2)$$

$$\beta_{11} m(0)^2 \equiv \frac{3(1-F)\sqrt{F}}{4\Omega Z^3 Y^2 A^2} \times \left\{ Z^{3/2} Y - 3(1-Z) \left[ \frac{1}{2\Omega} \sqrt{F} - \sqrt{Z} Y \right] \right\}, \quad (A3)$$

$$\beta_{01} m^2(0) \equiv S\dot{F} + T\dot{\Omega} + V\dot{A}, \quad (A4)$$

with

$$S \equiv \frac{-3\sqrt{F}}{4\Omega Y Z^{5/2} A} \left[ 1 + \frac{(3-2\Omega)(Z-F)}{4F\Omega Y} \right] \left( \frac{r}{a} \right),$$

$$T \equiv \frac{3(F/Z)^{1/2}(1-F)}{4ZY A \Omega^2} \left[ \frac{3[1 - (F/Z)^{1/2}]}{2\Omega Y} + 1 \right] \left( \frac{r}{a} \right),$$

$$V \equiv \frac{-3\sqrt{F}(1-F)}{2\Omega Z^{5/2} Y A^2} \left[ 1 + \frac{(3-2\Omega)(Z-F)}{4F\Omega Y} \right] \left( \frac{r}{a} \right)$$

$$+ \frac{3(1-F)^2}{4\Omega Z^2 Y^2 A^2} \left[ \frac{3}{2\Omega} - \frac{Y}{(F/Z)^{1/2}} \right] \left( \frac{r}{a} \right),$$

$$\tilde{m}_1 = \frac{3}{2} \frac{r^2}{a^2} (1-F), \quad (A5)$$

$$\frac{\tilde{m}_{12}}{r} m^2(0) = \frac{3(1-F)}{A^2}. \quad (\text{A6})$$

and

Feeding back (A1)–(A6) into (16) gives  $P$ . Then using the field equations one gets

$$\omega \equiv 1 - \frac{3(1-F)(F/Z)^{1/2}}{Y\Omega[3(1-F) + \bar{P}8\pi A^2]}, \quad (\text{A7})$$

$$\bar{\rho} \equiv \frac{3(1-F)(1+\omega)}{8\pi A^2} + \bar{P}\omega, \quad (\text{A8})$$

$$\bar{\epsilon} \equiv \frac{1}{8\Omega ZYA} \left[ \dot{F} + \frac{2(1-F)\dot{A}}{A} \right] \left( \frac{r}{a} \right)$$

$$+ \frac{(1-F)}{A^2} \left( \frac{3}{8\pi} \right) - \left( \frac{\bar{\rho} + \bar{P}\omega^2}{1-\omega^2} \right), \quad (\text{A9})$$

where  $\bar{P} \equiv Pm^2(0)$ ,  $\bar{\rho} \equiv \rho m^2(0)$ ;  $\bar{\epsilon} \equiv \epsilon m^2(0)$ .

## APPENDIX B

In the Tolman VI-type case, one arrives at the following expressions:

$$\tilde{m}_1 = \frac{1}{2}(1-F), \quad (\text{B1})$$

$$\tilde{m}_{11} = 0, \quad (\text{B2})$$

$$\beta = \frac{(1-F)}{3F} \ln \left\{ \left[ \frac{1 - \frac{1}{3}[(4\Omega-3)/(4\Omega-1)](r/a)}{1 - \frac{1}{3}[(4\Omega-3)/(4\Omega-1)]} \right]^2 \left( \frac{r}{a} \right) \right\}, \quad (\text{B3})$$

$$\beta_1 m(0) = \frac{(1-F)}{FA(r/a)} \left\{ \frac{(4\Omega-1) - (4\Omega-3)(r/a)}{3(4\Omega-1) - (4\Omega-3)(r/a)} \right\}, \quad (\text{B4})$$

$$\beta_{11} m^2(0) = \frac{(F-1)}{3FA^2(r/a)^2} \left\{ \frac{1 - \frac{2}{3}[(4\Omega-3)/(4\Omega-1)](r/a) + \frac{1}{3}[(4\Omega-3)/(4\Omega-1)]^2(r/a)}{[1 - \frac{1}{3}(4\Omega-3)/(4\Omega-2)](r/a)^2} \right\}. \quad (\text{B5})$$

<sup>1</sup>J. R. Oppenheimer and H. Snyder, *Phys. Rev.* **56**, 455 (1939).

<sup>2</sup>M. May and R. White, *Phys. Rev.* **141**, 1232 (1966).

<sup>3</sup>C. W. Misner and D. H. Sharp, *Phys. Rev.* **136**, B571 (1964).

<sup>4</sup>P. Vaidya, *Phys. Rev.* **83**, 10 (1951); *Astrophys. J.* **144**, 943 (1965).

<sup>5</sup>M. C. Faulkes, *Prog. Theor. Phys.* **42**, 1139 (1969).

<sup>6</sup>N. Chakravarty *et al.*, *Aust. J. Phys.* **29**, 113 (1976).

<sup>7</sup>D. Soares, *Phys. Rev. D* **17**, 1924 (1978).

<sup>8</sup>S. Bayin, *Phys. Rev. D* **19**, 2838 (1979).

<sup>9</sup>H. Bondi, *Proc. R. Soc. London* **A281**, 39 (1964).

<sup>10</sup>H. Bondi, M. G. J. Van der Burg, and A. W. K. Metzner, *Proc. R. Soc. London* **A269**, 21 (1962).

<sup>11</sup>In order to consider models which could be of physical interest, such as the Tolman VI-type model studied in Sec. VI, we do not impose regularity conditions such as  $\beta_1 = O(r)$ ,  $\tilde{m} = O(r^3)$  at  $r=0$ . Also, observe that negative pressures could appear at some stages of the contraction, so we do not require  $P \geq 0$ . See L. D. Landau and E. M. Lifshitz, *Statistical Physics* (Pergamon, New York, 1960).

<sup>12</sup>Observe that if one allows discontinuities of the radiation flux across the surface, then  $P_a$  is not necessarily zero. We are grateful to M. Demianski for this observation.

<sup>13</sup>R. Tolman, *Phys. Rev.* **55**, 364 (1939).